JOURNAL OF AGRICULTURAL AND FOOD CHEMISTRY

Article

Cite This: J. Agric. Food Chem. 2018, 66, 11663−11671

pubs.acs.org/JAFC

Discovery of TAS2R14 Agonists from *Platycodon grandiflorum* Using Virtual Screening and Affinity Screening Based on a Novel TAS2R14-Functionalized HEMT Sensor Combined with UPLC−MS Analysis

Zhi-Xin Wang,[†] Yu-Xin Zhang,[†] Yan-Ling Zeng,[†] Xi Li,[†] Zhao Chen,[†] Jia-Ming Luo,[‡] Yang Zhang,[‡] Yan-Ling Zhang,*[,†] and Yan-Jiang Qiao*[,†]

[†]Key Laboratory of TCM Information Engineering of State Administration of Traditional Chinese Medicine, Beijing University of Chinese Medicine, Beijing 102488, P. R. China

[‡]Key Laboratory of Semiconductor Materials Science, Chinese Academy of Sciences, Beijing 100083, P. R. China

Supporting Information

ABSTRACT: TAS2R14 is of great potential as a therapeutic target against asthma, and the discovery of TAS2R14 agonists can be very valuable for treating this disease. Herein, we developed a strategy using virtual screening and affinity screening based on a fabricated biosensor combined with UPLC−MS analysis to screen TAS2R14 agonists from *Platycodon grandiflorum*. By ligand-based virtual screening, 16 best-fit candidates were yielded. A novel TAS2R14-functionalized high-electron-mobility transistor (HEMT) sensor was applied to detect and fish out the potential TAS2R14 agonists from *P. grandiflorum* extracts. Those components captured by the immobilized TAS2R14 were eluted and characterized on UPLC−QTOF MS. As a result, six potential TAS2R14 agonists were screened out and identified. Among them, platycodin L was confirmed to be a special agonist of TAS2R14 for the first time and had an EC_{50} of 15.03 ± 1.15 μM via intracellular calcium mobilization assay (n = 6). The results indicated that the proposed strategy was efficient to discover TAS2R14 agonists from the herb directly.

KEYWORDS: *taste type 2 receptor 14 (TAS2R14), agonists, Platycodon grandiflorum, virtual screening, high-electron-mobility transistor (HEMT)*

INTRODUCTION

The bitter taste perception of human is mediated via taste type II receptors (TAS2Rs).[1] This kind of special G protein-coupled receptor (GPCR) was first discovered in gustatory cells and afterward in the extraoral system, where they play various physiological functions.[2] In particular, the expression and latent functions of TAS2Rs in respiratory tract have drawn broad concerns.[3−6] Previous investigations have proved that TAS2R14, the first identified one among the 25 subtypes of TAS2Rs, owns an exceptionally wide agonist spectrum[7−9] and the highest expression level in human bronchi.[10] Many TAS2R14 agonists, such as caffeine, quinine, and diphenidol have remarkable effects on the relaxation of airway smooth muscle, and they were thought to be promising drugs for asthma treatment clinically.[5,11] Therefore, TAS2R14 is of great potential as a therapeutic target against asthma, and the discovery of TAS2R14 agonists can be much valuable for treating this disease.

Traditional Chinese medicine (TCM) has served as an important source for the discovery of therapeutic agents over the past few decades.[12] *Platycodon grandiflorum* (Jacq.) A. DC., a kind of drug−food homologous plant, is widely distributed in China, Korea, and Japan. The dried root of *P. grandiflorum* was designated as "bitter taste" medicine according to the herbal property theory,[13] and it has been used to treat respiratory disease such as asthma,[14] airway inflammation,[15,16] and pulmonary tuberculosis,[13] so some chemical components in this herb are likely to be TAS2R14 agonists with potential clinical effects. High-throughput screening (HTS) is one of the dominant techniques for screening active ingredients from complex herb, but its applications in discovering the agonists of TAS2Rs are rare. Hu et al. fished out three TAS2R14 agonists from hundreds of natural compounds using the HTS model based on TAS2R14-overexpressed HEK293 cells.[17] However, this method will be effective only if a large bank of pure compounds is available; namely, HTS entails a huge separation workload and a low efficiency when using TCM as source. Hence, it is quite essential but challenging to develop an efficient and fast screening method for identifying agonists of TAS2Rs from TCM directly.

As a semiconductor device, AlGaAs/InGaAs-based high-electron-mobility transistor (HEMT) of the heterostructure shows characteristic electronic properties including piezoelectric and spontaneous polarization, which bring about a high density and migration rate of two-dimensional electron gas (2DEG) in its heterogeneous interface. Because that interface is very close to the surface of the device, any variance of surface conditions, such as binding outside molecules to the gate area, will significantly change the 2DEG density, which, in turn, alters the size of the interpolar current. Therefore, the HEMT can be taken as a powerful tool with ultrahigh sensitivity to detect bound substances.[18] Moreover, profiting from the advantages of a column packed with sub-2 μm particles,

Received: August 16, 2018
Revised: September 20, 2018
Accepted: September 27, 2018
Published: September 27, 2018

DOI: 10.1021/acs.jafc.8b04455
J. Agric. Food Chem. 2018, 66, 11663−11671

ultrahigh performance liquid chromatography (UPLC) enables efficient separation and saves analysis time.[19] High-resolution mass spectrometry (HRMS) has excellent qualitative ability, and the combination of UPLC with HRMS has become an extremely important technology in the field of natural product analysis more and more frequently.[20,21] In this study, an efficient strategy based on virtual screening and affinity screening by a novel TAS2R14-functionalized HEMT sensor combined with UPLC−MS analysis was proposed to fish out TAS2R14 agonists from *P. grandiflorum*. By ligand-based virtual screening, 16 best-fit candidates were first yielded. Then, TAS2R14 in membrane protein extracted from recombinational TAS2R14-overexpressed HEK293 cells was immobilized on an AlGaAs/InGaAs HEMT sensor to detect and capture the potential TAS2R14 agonists from *P. grandiflorum* extracts, followed by the two-step elution to release the bound agonists. The released components were collected and applied to UPLC−QTOF MS analysis for identification. As a result, six pentacyclic triterpenoid saponins including platycoside D, platycoside G2, platyconic acid A, platycodin D, platycodin L and platycodin K were identified and considered as the potential TAS2R14 agonists, which were also the hits in virtual screening. Among them, platycodin L was confirmed to be a special agonist of TAS2R14 for the first time and had an EC_{50} of 15.03 ± 1.15 μM via the intracellular calcium mobilization assay. This strategy could facilitate the research and development of effective antiasthmatic agents and provide a useful reference for screening the agonist or inhibitor class of drugs from TCM directly.

MATERIALS AND METHODS

Chemicals and Materials. Dulbecco's modified Eagle's medium (DMEM), fetal bovine serums (FBS), bull serum albumin (BSA), tris-buffered saline with Tween-20 (TBST), phosphate buffer solution (PBS, 100 mM, pH 7.4), Hank's balanced salt solution (HBSS), penicillin−streptomycin mixed solution (100×), hygromycin B, Geneticin (G418) and Mem-PER plus membrane protein extraction kit (89842) were purchased from Thermo Fisher Scientific (Waltham, MA, U.S.A.). The bicinchoninic acid protein assay (BCA) kit was from Biomiga (San Diego, CA, U.S.A.). Rabbit polyclonal anti-TAS2R14 antibody was from Abcam (Cambridge, U.K.). Rabbit monoclonal anti-Na^+/K^+-ATPase α_1 antibody was from Cell Signaling Technology (Boston, MA, U.S.A.). HRP-conjugated goat antirabbit IgG (H+L) secondary antibody was from TDY Biotechnology (Beijing, China).

Quinine, aristolochic acid, D-(−)-salicin, and platycodin D (purity ≥97%) were from Nature Standard Technology (Shanghai, China). Platycodin L (purity ≥98%) was from Quality Phytochemicals (East Brunswick, NJ, U.S.A.). Denatonium benzoate, probenecid, acid red 1,3-mercaptopropionic acid (3-MPA), 1-ethyl-3-(3-(dimethylamino)-propyl) carbodiimide hydrochloride (EDC) and *N*-hydroxysuccinimide (NHS) (all purity ≥98%) were from Sigma-Aldrich (St. Louis, MO, U.S.A.). Fluo-4 AM dye was from Molecular Probes (Grand Island, NY, U.S.A.). Matrigel was from Becton Dickinson (New York, U.S.A.). Methanol, acetonitrile, formic acid (UPLC grade), and dimethyl sulfoxide (DMSO, HPLC grade) were from Honeywell (Morris, NJ, U.S.A.). Deionized water was produced by the Millipore-Q water purification system (Millipore, Bedford, MA, U.S.A.).

P. grandiflorum was collected from Anhui, China in May 2016 (batch no. 16052904) and identified by Prof. Zhenfang Bai (School of Chinese Materia Medica, Beijing University of Chinese Medicine, Beijing, China). Voucher specimens were preserved at the authors' laboratory.

Establishment of Pharmacophore Model of TAS2R14 Agonists for Virtual Screening. Because of the unavailability of the 3D crystal structure of TAS2R14, the pharmacophore models of the TAS2R14 agonists were first established, and ligand-based virtual screening was adopted to predict the potential TAS2R14 agonists in *P. grandiflorum*, which could reduce the blindness of the following experimental procedure. Twelve known TAS2R14 agonists were used as a training set (Table S1) to establish pharmacophore models,[22] taking into account the structural diversity and activity of these compounds. The key steps for pharmacophore establishment were briefly described as follows.[23] The 3D pharmacophore hypotheses were constructed by HipHop (Common Feature Pharmacophore Generation) in Discovery Studio v4.0 (Accelrys, San Diego, CA). Conformations of ligand were generated within the relative energy threshold of 20 kcal/mol by BEST (Best Quality Conformer Generation) at the maximum size of 255 conformations. On the basis of initial analysis, hydrogen-bond acceptors (HBAs), hydrogen bond donors (HBDs), hydrophobic portions (HYs), and aromatic rings (ARs), which well-matched all of the training set ligands, have been selected. The interaction between ligand and receptor could be characterized by these pharmacophore features. The maximum number of pharmacophore models produced was set as 10. A decoy set, consisting of 37 experimentally known TAS2R14 agonists[22] (Table S2) and 191 nonactive compounds (Table S3), was applied to validate the established pharmacophore models. An empirical parameter CAI (comprehensive appraisal index) was used to quantify the capabilities of pharmacophore models.[23] The one with the highest CAI was picked as the query to screen the self-built 3D chemical database including 121 reported compounds derived from *P. grandiflorum* in Discovery Studio. The minimum interference distance was set as 1 Å, and the search algorithm was set as best. The other parameters were set as default. Finally, the fit values were calculated to denote the matching degree between the conformers of each compound and the pharmacophore model; namely, a higher fit value indicated a better match.

Construction of Recombinational TAS2R14−HEK293 Cells and Extraction of Membrane Protein with Overexpressed TAS2R14. To prepare the bioactive TAS2R14, a recombinational TAS2R14 ($G\alpha_{16}$gust44)−HEK293 cell line was constructed in which TAS2R14 was overexpressed. The coexistence of $G\alpha_{16}$ protein and gustducin of 44 amino acids was necessary for testing TAS2R14-agonistic activity in intracellular calcium mobilization assay.[24] A full-length human cDNA of TAS2R14 was first cloned and then cotransfected with the gene of $G\alpha_{16}$-gustducin into HEK293 cells.[24] Then, the recombinational TAS2R14−HEK293 cells were incubated in 5% CO_2 at 37 °C, and the medium was DMEM containing 10% FBS, 100 U/mL penicillin and 100 μg/mL streptomycin, 100 μg/mL hygromycin B, and 200 μg/mL G418. The last two kinds of antibiotics were used to inhibit the growth of nontransfected cells and consequently screen TAS2R14−HEK293 cells. Because of the existence of fluorescence tag within the constructed TAS2R14 expression vector, red fluorescence from stably growing TAS2R14−HEK293 cells should be easily observed under a fluorescence microscope (Figure S1). For comparison, primordial HEK293 cells were also cultured, but in DMEM, we just added 10% FBS, 100 U/mL penicillin and 100 μg/mL streptomycin. After sufficient cells were cultured and harvested, membrane fractions were extracted using the Mem-PER plus membrane protein extraction kit according to the suggested protocol.

Western Blotting for Identification and Quantification of TAS2R14. The concentration of extracted membrane protein was determined using the BCA kit. Then, Western blotting was adopted to identify TAS2R14 in recombinant TAS2R14−HEK293 cells and compare its content in membrane protein extracted from TAS2R14−HEK293 cells and HEK293 cells. Na^+/K^+-ATPase α_1 was used as the internal inference. The membrane fractions were first separated by SDS−PAGE and transferred to nitrocellulose membranes. After blocking with 3% BSA−TBST for 30 min, the membranes were incubated overnight in primary antibodies at 4 °C. The primary antibodies were rabbit polyclonal anti-TAS2R14 antibody and rabbit monoclonal anti-Na^+/K^+-ATPase α_1 antibody (both 1:5000 diluted with 3% BSA−TBST). After incubation, the membranes were exposed to HRP-conjugated goat antirabbit IgG (H+L) secondary antibody

DOI: 10.1021/acs.jafc.8b04455
J. Agric. Food Chem. 2018, 66, 11663−11671

(1:2000 diluted with 5% nonfat milk−TBST) for 40 min. Finally, the membranes were processed using the Chemistar High-sig ECL Western blotting substrate (Tanon, Shanghai, China) and analyzed on a GeneTex image analyzer (Fujifilm, Tokyo, Japan).

Fabrication of AlGaAs/InGaAs HEMT Sensor. The AlGaAs/InGaAs HEMT was grown by molecular beam epitaxy (MBE) on a GaAs substrate.[25] From bottom to top, it consisted of an undoped GaAs buffer layer (500 nm), an $In_{0.3}Ga_{0.7}As$ channel layer (15 nm), an $Al_{0.3}Ga_{0.7}As$ spacer layer (4 nm), a Si δ-doping layer, an $Al_{0.3}Ga_{0.7}As$ barrier layer (25 nm), and a GaAs cap layer (30 nm). Figure 1 shows the cross-sectional schematic drawing of the AlGaAs/InGaAs HEMT device. The detailed fabrication process of the HEMT was described in ref 26.

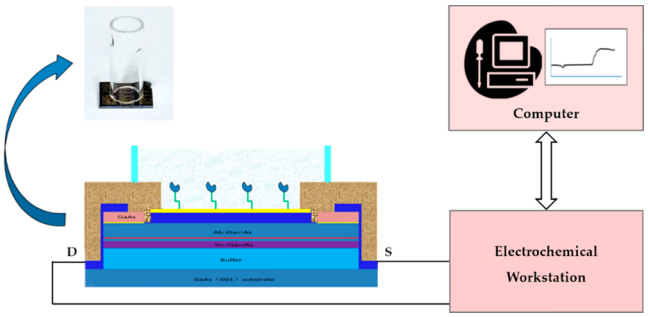

Figure 1. Measurement circuit of the fabricated AlGaAs/InGaAs HEMT-based biosensor sensor with a solution reservoir. The sensor chip is shown as a cross-sectional schematic drawing.

Immobilization of TAS2R14 on AlGaAs/InGaAs HEMT Sensor and XPS Characterization. Before the biofunctionalization process, a quartz glass tube (10 × 4 mm) was carefully stuck on the surface of the chip with "502" glue, which was used as a solution reservoir. The chip consisted of four groups of HEMT with 4 × 2 Au-coated gates just surrounded in the tube (Figure 1). Then 10 mM 3-MPA aqueous solution was added to the reservoir at room temperature for 24 h to form the self-assembled monolayer (SAM). After Au−S bonding, the sensor was washed with water to remove 3-MPA physically absorbed. Subsequently, a carboxyl activating aqueous solution containing equivoluminal 20 mM EDC and 50 mM NHS was dropped into the reservoir, reacted at room temperature for 15 min, and rinsed with 100 mM PBS. The activation reaction produced stable amine adducts.[27] Next, the extracted membrane protein containing overexpressed TAS2R14 was dissolved in 100 mM PBS (200 μg/mL) and introduced to the reservoir and incubated at 4 °C for 2 h, followed by washing.

XPS was carried out to characterize the immobilization of protein on Au-deposited GaAs substrates. XPS spectra were acquired by a K-Alpha XPS system (Thermo Fisher Scientific, U.S.A.) equipped with a monochromatic Al Kα source and a hemispherical electron energy analyzer. Low-resolution full scans (1 eV/step) and high-resolution fine scans (0.05 eV/step) of C 1s, N 1s, and S 2p were obtained, respectively. The software Avantage v5.965 (Thermo Fisher Scientific, U.S.A.) was employed to process XPS data.

Verification of Sensitivity and Response Range of TAS2R14-Functionalized HEMT Sensor. To determine the sensitivity and response range of the TAS2R14-functionalized HEMT sensor, the tests were performed using a quinine solution of 11 concentration gradients ranging from 0.1 pM to 1 mM as samples, and the HEMT sensor modified using membrane protein without overexpressed TAS2R14 was used as the negative control. Quinine was dissolved with 5% DMSO aqueous solution, which could fully dissolve the drug and minimize the damage to the activity of protein. The solvent was also used as the blank control throughout the experiment. Three minutes after adding drug solution to the reservoir, the measurement process was carried out on the probe platform. The drain-source current (I_{DS}) versus voltage (V_{DS}) of the biosensor was acquired at room temperature by a CHI-660E electrochemical workstation (Huake Putian Technology, Beijing, China). According to a previous experience, the biosensor would be broken down when V_{DS} exceeded 2 V, so the I_{DS} was measured in the V_{DS} scope of 0 to 2 V. Each test was repeated three times at each concentration. The I_{DS} at V_{DS} equal to 1 V was selected to calculate the relative I_{DS} and plot the response−concentration correlation.

Verification of Specificity of TAS2R14-Functionalized HEMT Sensor. Quinine and aristolochic acid are two known TAS2R14 agonists,[22] whereas D-(−)-salicin and denatonium benzoate are nonagonists.[8] In this investigation, the TAS2R14-functionalized HEMT sensor was exposed to solutions of these four bitter substances at 1 nM individually to further verify its specificity, and the HEMT sensor modified using membrane protein without overexpressed TAS2R14 was used as a negative control. All of the drugs for the test were also dissolved with 5% DMSO aqueous solution. After 3 min of reaction, I_{DS} versus V_{DS} was recorded in the scope of 0 to 2 V at room temperature, and every test was repeated three times. The I_{DS} at V_{DS} equal to 1 V was selected to calculate the relative I_{DS}.

Screening of Potential TAS2R14 Agonists from *P. grandiflorum* Using TAS2R14-Functionalized HEMT Sensor. Five hundred milligrams air-dried ground roots of *P. grandiflorum* were extracted by ultrasonic-assisted method with 25 mL of methanol for 30 min. The extracts was filtered and dried in vacuum, then redissolved in 25 mL of 5% DMSO aqueous solution and filtered through a 0.22 μm membrane as the sample.

Sixty microliters blank solvent and *P. grandiflorum* extracts sample were injected to the reservoir of the TAS2R14-functionalized HEMT sensor, respectively, and incubated at room temperature for 3 min, followed by scanning the I_{DS}−V_{DS} curve. After confirming the effective response derived from the bound ligands, the biosensor was washed with 60 μL of nonspecific eluent agent (100 mM PBS of pH 7.4) three times to remove any unbound components and then treated with 60 μL of specific eluent agent (1 μM quinine) for 3 min to release the captured potential TAS2R14 agonists. The released components were collected and then applied to UPLC−QTOF MS analysis for peak identification.

UPLC−QTOF MS Analysis and Identification for Potential TAS2R14 Agonists. The components eluted from the biosensor were analyzed on an Agilent 1260 Infinity UPLC coupled to an Agilent 6540 Exact Mass QTOF MS system (Agilent, Santa Clara, CA, U.S.A.). The column used for separation was an Agilent Zorbax RRHD Eclipse Plus C_{18} column (100 × 3.0 mm, 1.8 μm; Agilent, U.S.A.), which performed at 40 °C. The mobile phase consisted of solvent A (0.5% formic acid in water, v/v) and solvent B (acetonitrile) using a gradient elution program as follows: 30−50% B at 0−5 min. The flow rate was kept at 0.4 mL/min. The sample volume injected was set at 2 μL. Mass analysis was carried out in negative ESI mode, and the parameters of the ion source were set as follows: drying gas temperature, 200 °C; drying gas flow rate, 11 L/min; nebulizer pressure, 35 psig; sheath gas flow rate, 9 L/min; sheath gas temperature, 225 °C; capillary voltage, 3500 V; nozzle voltage, 1000 V; fragmentor voltage, 380 V; and Oct 1 RF Vpp, 750 V. The acquired mass range was set at m/z 100−1500 Da. All other MS parameters were left as default settings. The software Agilent MassHunter Qualitative Analysis B07.00 (Agilent, U.S.A.) was applied for MS data processing. The components identification was conducted through the process of generating molecular formulas on the basis of m/z values of quasi-molecular ions, searching reported compounds in the genus of *Platycodon* and confirming targeted structures. The threshold of mass error was fixed at 3 ppm.

Evaluation for Screened TAS2R14 Agonists by Intracellular Calcium Mobilization Assay. The intracellular calcium mobilization assay was employed to evaluate the TAS2R14-agonistic activity of those potential agonists. However, due to the unavailability of standard substances of the other four compounds, only platycodin D and platycodin L were applied in this assay. The two different drugs were dissolved in DMSO at 100 mM, and 8 μM aristolochic acid and 0.25% DMSO were used as the positive and negative controls, respectively. The final concentration of DMSO in each well did not exceed 0.25% for all of the tested drugs. The TAS2R14−HEK293

DOI: 10.1021/acs.jafc.8b04455
J. Agric. Food Chem. 2018, 66, 11663−11671

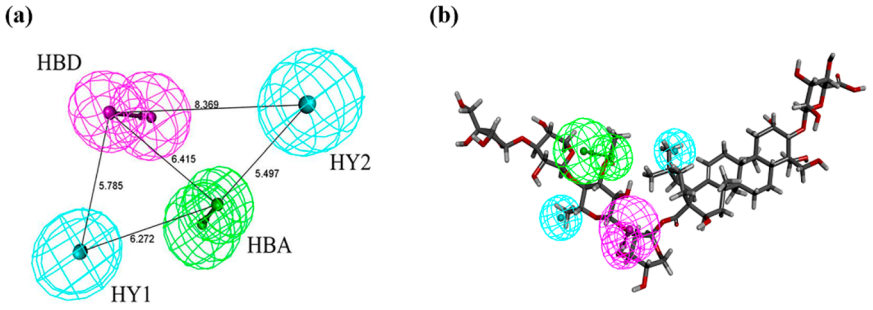

Figure 2. Optimal pharmacophore model of special TAS2R14 agonists and match mode of the best-fit candidate platycodin L. (a) Model-01, the optimal pharmacophore model of special TAS2R14 agonists. The numbers represent the distance between two pharmacophore features. The arrows represent the direction of hydrogen bonds. Gray, white, red, blue, and yellow spheres represent carbon, hydrogen, oxygen, nitrogen and sulfur atoms, respectively. HY: hydrophobic portion; HBD: hydrogen bond donor; HBA: hydrogen bond acceptor. (b) Match mode of the best-fit candidate platycodin L in the pharmacophore model of special TAS2R14 agonists.

cells were seeded into 96-well plates coated with Matrigel at a density of 3.0×10^4/well and cultured in 5% CO_2 at 37 °C overnight. Before assay, the medium in each well was substituted by 100 μL of loading buffer containing 4 μM Ca^{2+}-sensitive Fluo-4 AM dye, 2.5 mM probenecid and 2 mM acid red 1 in HBSS. The plate was then incubated in the dark for 30 min before detecting the calcium signal. For studying the antagonism, 80 μL of loading buffer was complemented to each well, together with 20 μL of HBSS containing tested drugs with a suitable concentration 10 min before calcium-flux detection. Cells were transferred to a FlexStation III (Molecular Devices, San Jose, CA, U.S.A.) for fluorescence scanning. Basal fluorescence was scanned for 16 s prior to application of the agonist. Then, the integrated fluidics system of FlexStation III transferred 25 μL of drug solution from the drug plate to the assay plate, which contained 100 μL of loading buffer. The relative fluorescence units (RFUs) were recorded at 37 °C at an excitation wavelength of 485 nm and emission wavelength of 525 nm, every 2 s for 100 s. At last, the EC_{50} value was calculated by RFU. Each datum represents the mean ± standard deviation in six replicates.

A specificity assay was performed to eliminate the false-positive results in the activity evaluation. If a drug exhibited an equivalent ability to induce intracellular calcium-influx in both HEK293 cells and TAS2R14−HEK293 cells, then it would be thought of as the false-positive. Herein, HEK293 cells were treated with platycodin D and platycodin L of various concentrations to observe whether they could induce calcium influx. The positive and negative controls were the same as in the above assay.

Statistical Tests. All data acquired in the performance characterization of the biosensor and the intracellular calcium mobilization assay were processed using one-way analysis of variance (ANOVA), followed by Student's *t*−test to find the differences between group means in GraphPad Prism v7.0 (GraphPad Software, La Jolla, CA, U.S.A.); $p < 0.05$ was considered significant, and $p < 0.01$ denoted very significant.

RESULTS AND DISCUSSION

Virtual Screening for Potential TAS2R14 Agonists in *P. grandiflorum*. Ten pharmacophore models of TAS2R14 agonists were established and evaluated (see Table S4). Model-01 (Figure 2a) had the highest CAI, so it was the optimal pharmacophore and was used to predict active compounds. As a result, the calculation produced a list of 16 candidates from *P. grandiflorum*, which had higher fit values than the positive drug quinine (Table 1). Among the candidates, except for quercetin-7-*O*-rutinoside, all of them belonged to pentacyclic triterpenoid saponins, which were made up of pentacyclic triterpenoids and glycosyl units. As their key structural characteristic, it is the various glycosyls that largely determined the fit values. Platycodin L showed the highest fit value of 3.247, of which the glycosyls were Glc (at R_1) and ^{1}Ara^2-^{1}Rha (Ac-O-3)^4-^{1}Xyl^3-^{1}Api (at R_3), respectively (Figure 2b).

Table 1. Sixteen Candidates and Their Corresponding Fit Values Calculated from Ligand-Based Virtual Screening

ID	molecular formula	compound name	fit value[a]
01	$C_{59}H_{92}O_{30}$	platycodin L	3.247
02	$C_{27}H_{30}O_{16}$	quercetin-7-*O*-rutinoside	3.215
03	$C_{59}H_{92}O_{30}$	platycodin K	3.115
04	$C_{57}H_{92}O_{28}$	platycodin D	3.100
05	$C_{64}H_{104}O_{33}$	platycoside I	3.031
06	$C_{59}H_{96}O_{30}$	platycoside G2	2.998
07	$C_{52}H_{80}O_{54}$	platycoside M3	2.988
08	$C_{52}H_{84}O_{23}$	platycoside J	2.973
09	$C_{38}H_{60}O_{13}$	dimethyl-3-*O*-*β*-D-glucopyranosyl platycogenate A	2.918
10	$C_{36}H_{58}O_{12}$	3-*O*-*β*-D-glucopyranosyl platycodigenin	2.918
11	$C_{69}H_{112}O_{37}$	platycoside D	2.913
12	$C_{57}H_{90}O_{28}$	16-oxo-platycodin D	2.868
13	$C_{37}H_{60}O_{11}$	methyl 3-*O*-*β*-D-glucopyranosyl polygalacate	2.842
14	$C_{58}H_{94}O_{28}$	platycoside H	2.830
15	$C_{57}H_{90}O_{29}$	platyconic acid A	2.794
16	$C_{47}H_{76}O_{20}$	platycoside F	2.774
positive drug	$C_{20}H_{24}N_2O_2$	quinine	2.746

[a]Fit value is a score to evaluate the fitness and dependence on the proximity of the features to pharmacophore centroids and the weights assigned to each feature. The larger this value is, the better the match is.

Quantification of TAS2R14 in Extracted Membrane Protein. The concentration of extracted membrane protein determined by BCA kit was 940 μg/mL. As the Western blotting results shown in Figure 3, the isolated bands of

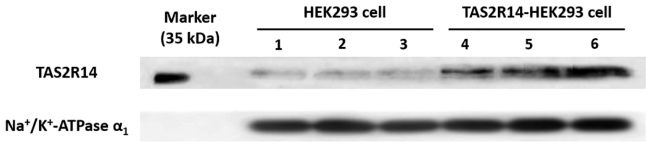

Figure 3. Comparison of Western blotting results of TAS2R14 in membrane protein extracted from HEK293 cells and TAS2R14−HEK293 cells. Na^+/K^+-ATPase α_1 was used as the internal reference.

DOI: 10.1021/acs.jafc.8b04455
J. Agric. Food Chem. 2018, 66, 11663−11671

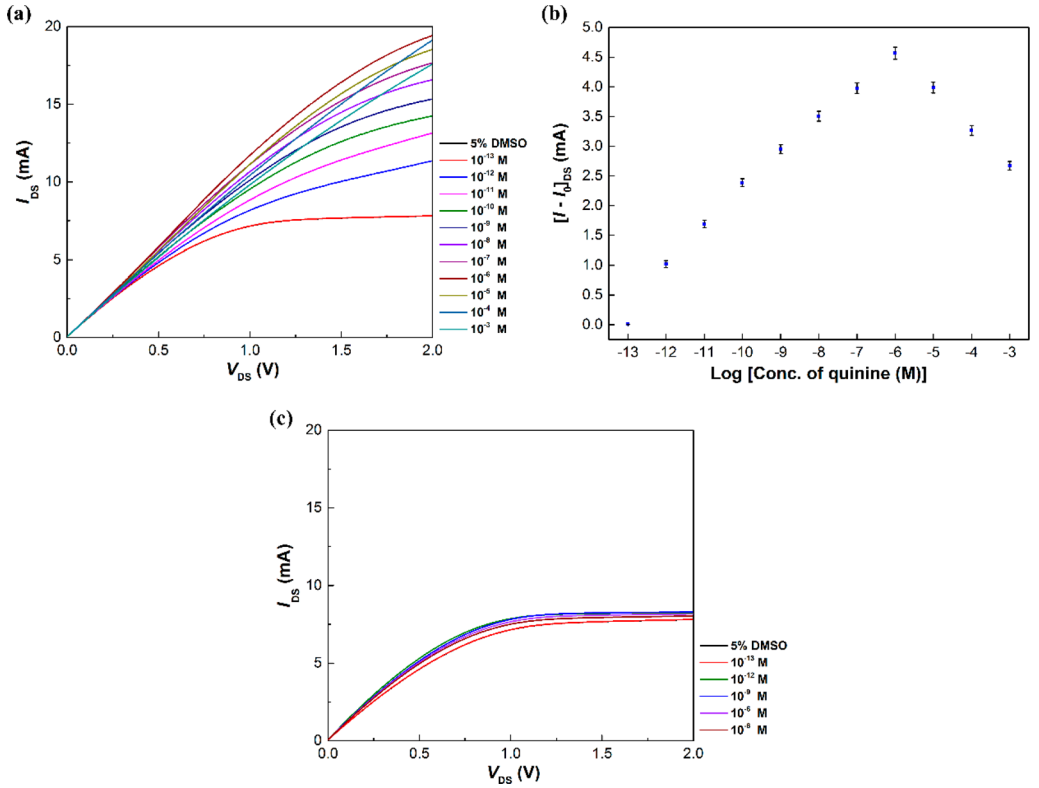

Figure 4. Sensitivity and response range of TAS2R14-functionalized HEMT sensor. (a) Current versus voltage with TAS2R14-functionalized HEMT sensor successively exposed to quinine of different concentrations ranging from 0.1 pM to 1 mM (5% DMSO was blank control). (b) Relative current with a voltage of 1 V versus quinine concentration ranging from 0.1 pM to 1 mM on log scale. All data are presented as mean ± standard deviation in three independent experiments. (c) Current versus voltage with negative control HEMT sensor modified using membrane protein without overexpressed TAS2R14 exposed to quinine of five concentrations ranging from 0.1 pM to 1 mM.

targeted protein that appeared at the region above 35 kDa showed that TAS2R14 (36.2 kDa) was expressed in both of those two kinds of cells and enriched successfully in the extracted membrane protein. The relative grayscales of TAS2R14 bands to Na^+/K^+-ATPase α_1 bands in membrane protein extracted from TAS2R14−HEK293 cells and HEK293 cells were 0.118 ± 0.017 and 0.020 ± 0.003, respectively. This indicated that the content of TAS2R14 extracted from TAS2R14−HEK293 cells was approximately six times than that from HEK293 cells.

Verification of TAS2R14 Immobilization on AlGaAs/InGaAs HEMT Sensor. To verify the SAM formation and TAS2R14 immobilization on the gate, the XPS spectra were analyzed. Before the modification of the Au surface, only photoelectron peaks corresponding to the elements in the chip were observed, except for the C 1s peak,[28] as shown in Figure S1a. After the 3-MPA reaction, a new peak at 162.5 eV (S 2p) from thiol of 3-MPA occurred (Figure S1b). The upper right inset shows the high-resolution spectra of S 2p. The S 2p peak was decomposed and assigned to bound thiolate and unbound thiol.[29] The chip was then immersed into membrane protein solution containing TAS2R14. The spectra of the TAS2R14-adsorbed chip are shown in Figure S1c. The N 1s peak at 400.0 eV indicated the amine of the protein, which could be used to indirectly quantify protein.[30] From the above results, we could affirm that the SAM was formed on the gate, and the TAS2R14 was immobilized via SAM.

Figure S2 shows the high-resolution spectra of N 1s and C 1s for untreated, SAM-formed and TAS2R14-immobilized chip, respectively. The deconvolution of peaks is depicted in dotted lines. The N 1s peak appeared after protein coupling. It could be decomposed into two subpeaks, centered at 401.3 and 403.5 eV, respectively, which corresponded to the neutral (NH_2) and protonated (NH_3^+) forms of amino in protein.[31] The C 1s spectra of untreated chip were assigned to two peaks at 284.9 (C−H) and 286.2 eV (C−O). The carbon signal came from common element in substrates because of organic contaminations.[28] After SAM formed, a new peak occurred at 289.0 eV, which indicated the introduction of carboxyl (O−C═O).[32] The carboxyl was then activated by NHS/EDC and bonded to amino of protein.[27] After the sample was immersed into membrane protein solution containing plenty of TAS2R14, the C 1s spectra became broader due to the formation of peptide bond (−CONH−) at 286.5 eV.[33]

Sensitivity and Response Range of TAS2R14-Functionalized HEMT Sensor. As shown in Figure 4a, in the range of quinine concentration from 0 to 1 mM, TAS2R14-functionalized HEMT sensor showed a typical volt−ampere characteristic curve of the semiconductor. As the quinine concentration increased, the slope of the $I_{DS}-V_{DS}$ curve changed regularly. It was proved that the electrical property of the biosensor was influenced by quinine because of the change of 2DEG concentration in the channel layer of the gate region. After the quinine concentration exceeded 1 mM, the biosensor was overloaded and completely became a conductor. Figure 4b exhibited the relative I_{DS} at V_{DS} equal to 1 V versus quinine concentration ranging from 0.1 pM to 1 mM on a log scale. It was obvious from the results that the biosensor started to show a significant response when the quinine concentration reached 1 pM; namely, the lowest detection concentration of biosensor

DOI: 10.1021/acs.jafc.8b04455
J. Agric. Food Chem. 2018, 66, 11663−11671

for quinine could be as lows as 1 pM. In the concentration range of 1 pM to 1 μM, the relative I_{DS} was positively correlated with the logarithm of the concentration, which was just the linear response range of biosensor. As a result of the saturation of TAS2R14, the response decreased linearly after quinine concentration exceeded 1 μM. As a contrast, Figure 4c is the $I_{DS}-V_{DS}$ curve of the negative control HEMT sensor modified using membrane protein without overexpressed TAS2R14 exposed to quinine of different concentration ranging from 0.1 pM to 1 mM, which displayed no significant response. This result demonstrated that the biosensor is strictly TAS2R14-dependent.

Specificity of TAS2R14-Functionalized HEMT Sensor. As shown in Figure 5, the biosensor modified with membrane protein containing overexpressed TAS2R14 had a significantly higher and specific response to quinine and aristolochic acid and no significant response to D-(−)-salicin and denatonium benzoate ($p < 0.01$). The much smaller response of D-(−)-salicin and denatonium benzoate could originate from the nonspecific adsorption of bitter substances onto the sensor surface, whereas the negative control biosensor modified using membrane protein without overexpressed TAS2R14 showed very low response to all bitter stimuli tested. All of the results demonstrated the high specificity of TAS2R14-functionalized HEMT sensor for the detection of TAS2R14 agonists.

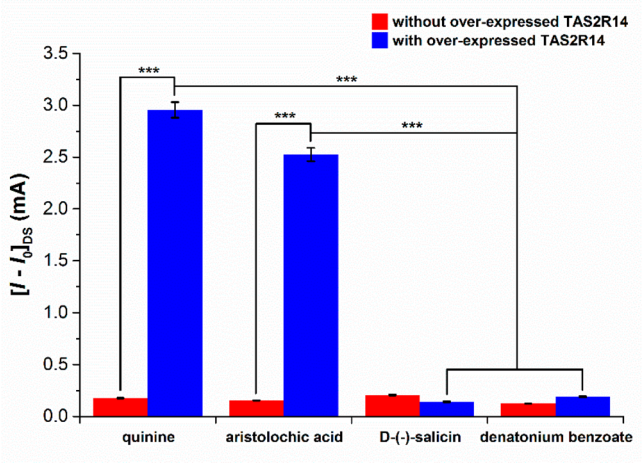

Figure 5. Responses of HEMT sensors functionalized with different sensitive elements (membrane protein with/without overexpressed TAS2R14) to various bitter stimuli at 1 nM (quinine, aristolochic acid, D-(−)-salicin and denatonium benzoate). All relative I_{DS} values were presented as mean ± standard deviation in three independent experiments. *** $p < 0.01$, Student's t−test.

Screening and Identification of Potential TAS2R14 Agonists from *P. grandiflorum*. After verifying the sensitivity, responding range and specificity, the TAS2R14-functionalized HEMT sensor was used to detect and screen the potential TAS2R14 agonists from *P. grandiflorum* extracts. When exposed to herb sample from 5% DMSO aqueous solution, the TAS2R14-functionalized HEMT sensor showed a significant response, whereas the negative control sensor modified using the membrane protein without overexpressed TAS2R14 had no significant response (Figure 6). This indicated that the potential agonists in *P. grandiflorum* were effectively recognized and captured by TAS2R14. After washed with 100 mM PBS, any unbound components were removed from the surface of receptors. Then, treated with 1 μM quinine, the response further increased because stronger binding between plenty of quinine and receptors happened naturally. As a result, those potential agonists derived from herb with relative weak binding force were replaced by quinine and released into the solution. Of course, the elution power of quinine was also limited. Those ligands with stronger binding than quinine could still stay on the surface of receptors, the release of which required more powerful eluents such as flufenamic acid.[8] As a methodological exploration, quinine was tentatively used to conduct experiments in the current study.

The released components were analyzed using UP-LC−QTOF MS, followed by peaks identification. As a result, eight pentacyclic triterpenoid saponins in the eluent were finally identified (Figure 7; see Table S5). Especially among them, six compounds including platycoside D, platycoside G2, platyconic acid A, platycodin D, platycodin L, and platycodin K were also the best-fit candidates in the virtual screening. Thus, they were considered to be the potential TAS2R14 agonists.

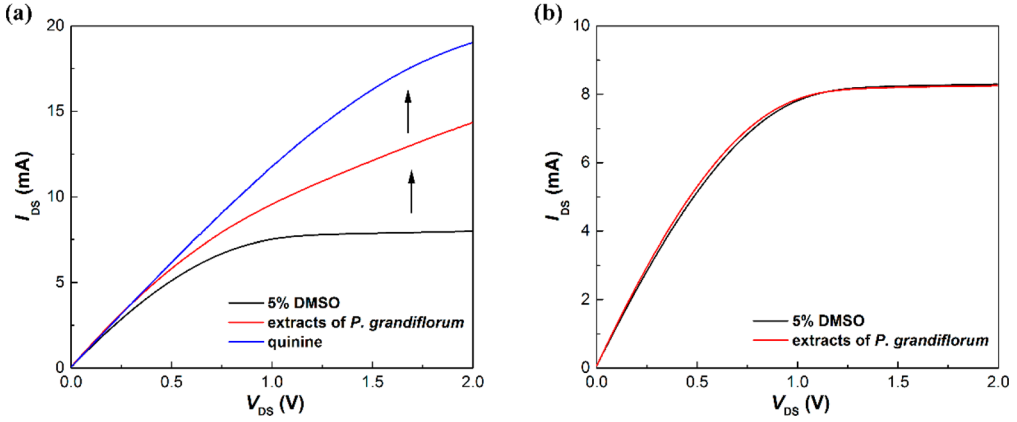

Figure 6. Potential TAS2R14 agonists in *P. grandiflorum* were effectively captured by TAS2R14 and released after the two-step elution process. (a) TAS2R14-functionalized HEMT sensor showed a significant response when exposed to a sample of *P. grandiflorum* extracts from 5% DMSO aqueous solution (blank), and the response further increased after it was washed with 100 mM PBS and treated with 1 μM quinine. (b) Negative control HEMT sensor modified using membrane protein without overexpressed TAS2R14 had no significant response to sample of *P. grandiflorum* extracts.

DOI: 10.1021/acs.jafc.8b04455
J. Agric. Food Chem. 2018, 66, 11663−11671

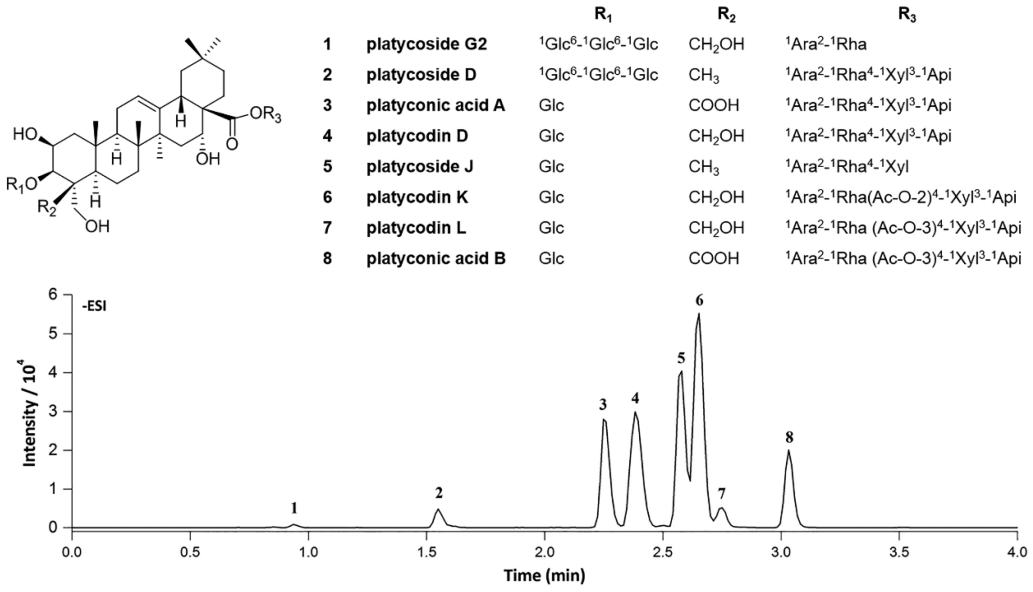

Figure 7. Chemical structures of the eight identified components in the eluent and their corresponding peaks on TIC chromatogram in negative ESI mode.

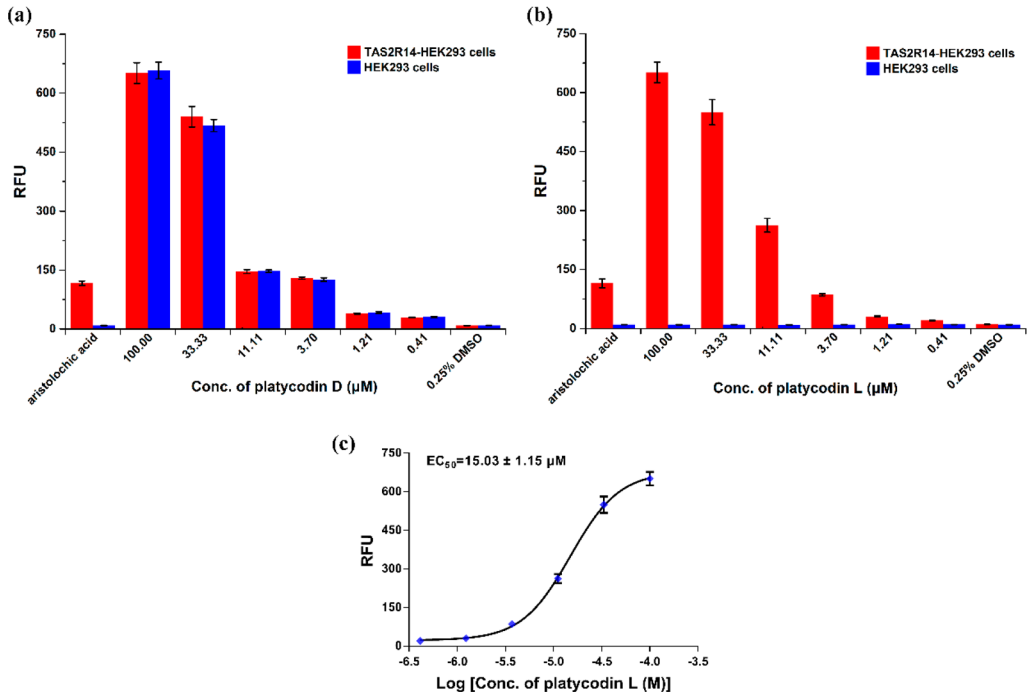

Figure 8. Evaluation of the agonistic activity and specificity of two screened TAS2R14 agonists by the intracellular calcium mobilization assay. Calcium-influx responses were compared when TAS2R14−HEK293 cells and HEK293 cells were treated with different concentrations of platycodin D (a) and platycodin L (b). Aristolochic acid (8 μM) and 0.25% DMSO were used as the positive and negative controls, respectively. RFU (relative fluorescence unit) means the difference in relative fluorescence units between the maximum and the minimum. All error bars indicate the standard deviation in six replicates. (c) EC_{50} value of platycodin L was calculated from the logarithmic concentration−response curve as 15.03 ± 1.15 μM. All error bars indicate the standard deviation in six replicates.

Agonistic Activity and Specificity of Screened TAS2R14 Agonists. The agonistic activities of two screened TAS2R14 agonists, platycodin D and platycodin L, were effectively evaluated by an intracellular calcium mobilization assay on the established TAS2R14−HEK293 cell line. The results indicated that both platycodin D and platycodin L showed significantly enhanced calcium-influx signals compared with the control group ($p < 0.05$) in TAS2R14−HEK293 cells (Figure 8a,b). To further evaluate the specificity, an intracellular calcium mobilization assay on HEK293 cells was also conducted. Compared with 0.25% DMSO, platycodin D showed significant calcium-influx signals in HEK293 cells (Figure 8a), whereas platycodin L did not show any effect (Figure 8b). It could be deduced from the results that the evoked Ca^{2+} was the second messenger triggered when TAS2R14 was exposed to platycodin L. Thus platycodin L was determined to be a specific TAS2R14 agonist, of which the EC_{50} value was 15.03 ± 1.15 μM in six replicates (Figure 8c).

DOI: 10.1021/acs.jafc.8b04455
J. Agric. Food Chem. 2018, 66, 11663−11671

However, platycodin D showed the nonspecific agonistic activity to TAS2R14, and the calcium-influx induced by it was a false-positive result.

For reducing the costs, the biorecognition element used in constructed biosensor was the extracted membrane protein. Although TAS2R14 was overexpressed, there were still other receptors in membrane protein. Some high-content chemical components such as platycodin D in the sample could be bound to other receptors and eluted by quinine. Therefore, the appearance of a false-positive was inevitable, even when applying more powerful eluents. In this case, the activity evaluation based on intracellular calcium mobilization assay for screened potential TAS2R14 agonists was necessary, which could ensure the reliability of this strategy. In the future investigation, the biosensor could be constructed with purified TAS2R14, or the content of TAS2R14 in the extracted membrane protein could be further improved to reduce the probability of a false-positive.

In summary, we have developed an efficient strategy for screening TAS2R14 agonists from herb extracts directly, which was a hybrid combination of ligand-based virtual screening, affinity screening based on TAS2R14-functionalized HEMT sensor, as well as following a two-step elution process and UPLC−QTOF MS analysis. One of the six yielded potential agonists, platycodin L, was confirmed by an intracellular calcium mobilization assay for the first time to be a special agonist of TAS2R14. More pharmacological studies will be conducted to verify the activities of other potential TAS2R14 agonists once the compounds are available. The current methodology could facilitate the research and development of effective antiasthmatic agents and provide a useful reference for directly screening agonists or inhibitor classes of drugs from the complex matrix.

■ ASSOCIATED CONTENT

Supporting Information

The Supporting Information is available free of charge on the ACS Publications website at DOI: 10.1021/acs.jafc.8b04455.

Table S1. 12 experimentally known TAS2R14 agonists used as a training set to establish the pharmacophore models. Table S2. 37 experimentally known TAS2R14 agonists used as a decoy set to validate the established pharmacophore models. Table S3. 191 nonactive compounds used as a decoy set to validate the established pharmacophore models. Table S4. All established pharmacophore models of TAS2R14 agonists for virtual screening and their performance parameters. Table S5. Eight identified or tentatively identified components from the eluent and their UPLC−QTOF MS data. Figure S1. Fluorescence images of recombinational TAS2R14−HEK293 cells and primordial HEK293 cells (both unstained). Figure S2. XPS spectra obtained with the Au deposited substrate: no treatment, after 3-MPA immobilization, and after membrane protein containing TAS2R14 adsorption. Figure S3. High-resolution XPS spectra of N 1s and C 1s. (PDF)

■ AUTHOR INFORMATION

Corresponding Authors

*Y.-J.Q.: Phone: 086-10-84738661. E-mail: yjqiao@263.net.

*Y.-L.Z.: Phone: 086-10-84738662. E-mail: collean_zhang@163.com.

ORCID

Zhi-Xin Wang: 0000-0001-7255-6049

Author Contributions

Y.-J.Q., Y.-L.Z., and Z.-X.W. designed the research. Z.-X.W. carried out the experiments and wrote the manuscript. Y.-X.Z., Y.-L.Z., X.L., and Z.C. commented on the experiments and manuscript. J.-M.L. and Y.Z provided guidance for the fabrication and modification of sensor. All authors read and approved the final manuscript.

Funding

This work was supported by Project Funded by China Postdoctoral Science Foundation (2017M620701) and National Natural Science Foundation of China (81430094).

Notes

The authors declare no competing financial interest.

■ ACKNOWLEDGMENTS

The assistance of Dr. Xing Wang of Capital Medical University for the virtual screening is acknowledged.

■ REFERENCES

(1) Chandrashekar, J.; Mueller, K. L.; Hoon, M. A.; Adler, E.; Feng, L.; Guo, W.; Zuker, C. S.; Ryba, N. J. P. T2Rs function as bitter taste receptors. *Cell* **2000**, *100*, 703−711.

(2) Kinnamon, S. C. Taste receptor signalling - from tongues to lungs. *Acta Physiol.* **2012**, *204*, 158−168.

(3) Sanderson, M. J.; Madison, J. M. Bitter treats for better breathing. *Nat. Med.* **2010**, *16*, 1190−1191.

(4) Lee, R. J.; Xiong, G. X.; Kofonow, J. M.; Chen, B.; Lysenko, A.; Jiang, P. H.; Abraham, V.; Doghramji, L.; Adappa, N. D.; Palmer, J. N.; Kennedy, D. W.; Beauchamp, G. K.; Doulias, P. T.; Ischiropoulos, H.; Kreindler, J. L.; Reed, D. R.; Cohen, N. A. T2R38 taste receptor polymorphisms underlie susceptibility to upper respiratory infection. *J. Clin. Invest.* **2012**, *122*, 4145−4159.

(5) Grassin-Delyle, S.; Abrial, C.; Fayad-Kobeissi, S.; Brollo, M.; Faisy, C.; Alvarez, J. C.; Naline, E.; Devillier, P. The expression and relaxant effect of bitter taste receptors in human bronchi. *Resp. Res.* **2013**, *14*, 134.

(6) Lee, R. J.; Kofonow, J. M.; Rosen, P. L.; Siebert, A. P.; Chen, B.; Doghramji, L.; Xiong, G. X.; Adappa, N. D.; Palmer, J. N.; Kennedy, D. W.; Kreindler, J. L.; Margolskee, R. F.; Cohen, N. A. Bitter and sweet taste receptors regulate human upper respiratory innate immunity. *J. Clin. Invest.* **2014**, *124*, 1393−1405.

(7) Behrens, M.; Brockhoff, A.; Kuhn, C.; Bufe, B.; Winnig, M.; Meyerhof, W. The human taste receptor hTAS2R14 responds to a variety of different bitter compounds. *Biochem. Biophys. Res. Commun.* **2004**, *319*, 479−485.

(8) Meyerhof, W.; Batram, C.; Kuhn, C.; Brockhoff, A.; Chudoba, E.; Bufe, B.; Appendino, G.; Behrens, M. The molecular receptive ranges of human TAS2R bitter taste receptors. *Chem. Senses* **2010**, *35*, 157−170.

(9) Levit, A.; Nowak, S.; Peters, M.; Wiener, A.; Meyerhof, W.; Behrens, M.; Niv, M. Y. The bitter pill: clinical drugs that activate the human bitter taste receptor TAS2R14. *FASEB J.* **2014**, *28*, 1181−1197.

(10) Deshpande, D. A.; Wang, W. C. H.; Mcilmoyle, E. L.; Robinett, K. S.; Schillinger, R. M.; An, S. S.; Sham, J. S. K.; Liggett, S. B. Bitter taste receptors on airway smooth muscle bronchodilate by localized calcium signaling and reverse obstruction. *Nat. Med.* **2010**, *16*, 1299−1304.

(11) Sharma, P.; Yi, R.; Nayak, A. P.; Wang, N.; Tang, F.; Knight, M. J.; Pan, S.; Oliver, B.; Deshpande, D. A. Bitter taste receptor agonists mitigate features of allergic asthma in mice. *Sci. Rep.* **2017**, *7*, 46166.

DOI: 10.1021/acs.jafc.8b04455
J. Agric. Food Chem. 2018, 66, 11663−11671

(12) Lin, Y.; Betz, J. M.; Bindra, J. S.; Bobzin, S. C. *Drug Discovery and Traditional Chinese Medicine: Science, Regulation, and Globalization*; Springer: New York, 2001.
(13) Nanjing University of Chinese Medicine. *Dictionary of Chinese Materia Medica*, 2nd ed.; Shanghai Science and Technology Press: Shanghai, China, 2006; pp 2526−2527.
(14) Yu, W. Y.; Zhu, H. J. Pharmacological mechanism of *Platycodon grandiflorum* on treatment of bronchial asthma. *Acta Chin. Med. Pharmacol.* **2012**, *40*, 38−40.
(15) Choi, J. H.; Hwang, Y. P.; Lee, H. S.; Jeong, H. G. Inhibitory effect of *Platycodi Radix* on ovalbumin-induced airway inflammation in a murine model of asthma. *Food Chem. Toxicol.* **2009**, *47*, 1272−1279.
(16) Choi, J. H.; Jin, S. W.; Kim, H. G.; Choi, C. Y.; Lee, H. S.; Ryu, S. Y.; Chung, Y. C.; Hwang, Y. J.; Um, Y. J.; Jeong, T. C.; Jeong, H. G. Saponins, especially Platyconic acid A, from *Platycodon grandiflorum* reduce airway inflammation in ovalbumin-induced mice and PMA-exposed A549 cells. *J. Agric. Food Chem.* **2015**, *63*, 1468−1476.
(17) Hu, Y. X.; Cai, W.; Zhang, H. H.; Yu, C. H.; Yu, W. Y.; Jin, X. Y.; Ying, H. Z. Establishment and application of screening model for anti-asthmatic natural active ingredients based on bitter taste receptors in lung tissue. *Chin. Tradit. Herb. Drugs* **2016**, *47*, 775−780.
(18) Kang, B. S.; Wang, H. T.; Ren, F.; Pearton, S. J. Electrical detection of biomaterials using AlGaN/GaN high electron mobility transistors. *J. Appl. Phys.* **2008**, *104*, 031101.
(19) Yi, T.; Tang, Y.; Zhang, J.; Zhao, Z.; Yang, Z.; Chen, H. Characterization and determination of six flavonoids in the ethnomedicine ″Dragon's Blood″ by UPLC-PAD-MS. *Chem. Cent. J.* **2012**, *6*, 116.
(20) Zhu, L.; Han, Q.; Ho, A.; Hsiao, W.; Jiang, Z. Characterization and simultaneous determination of immunosuppressive decalins in red yeast rice by ultra-high-performance liquid chromatography hyphenated with mass spectrometry. *J. Chromatogr. A* **2013**, *1303*, 54−61.
(21) Chen, Q.; Zhu, L.; Tang, Y.; Kwan, H.; Zhao, Z.; Chen, H.; Yi, T. Comparative evaluation of chemical profiles of three representative 'snow lotus' herbs by UPLC-DAD-QTOF-MS combined with principal component and hierarchical cluster analyses. *Drug Test. Anal.* **2017**, *9*, 1105−1115.
(22) Wiener, A.; Shudler, M.; Levit, A.; Niv, M. Y. BitterDB: a database of bitter compounds. *Nucleic Acids Res.* **2012**, *40*, 413−419.
(23) Wang, X.; Xiang, Y. H.; Ren, Z. Z.; Zhang, Y. L.; Qiao, Y. J. Rational questing for inhibitors of endothelin converting enzyme-1 from *Salvia miltiorrhiza* by combining ligand- and structure-based virtual screening. *Can. J. Chem.* **2013**, *91*, 448−456.
(24) Ueda, T.; Ugawa, S.; Yamamura, H.; Imaizumi, Y.; Shimada, S. Functional interaction between T2R taste receptors and G-Protein α subunits expressed in taste receptor cells. *J. Neurosci.* **2003**, *23*, 7376−7380.
(25) Cui, L. J.; Zeng, Y. P.; Wang, B. Q.; Zhu, Z. P.; Guo, S. L.; Chu, J. H. Correlation between optical and electrical properties in In0.52Al0.48As/InxGa1-xAs metamorphic high-electron-mobility-transistor structures on GaAs substrates. *J. Appl. Phys.* **2006**, *100*, 033705.
(26) Niu, J. Q.; Zhang, Y.; Guan, M.; Wang, C. Y.; Cui, L. J.; Yang, Q. M.; Li, Y. Y.; Zeng, Y. P. Detection of lead ions with AlGaAs/InGaAs pseudomorphic high electron mobility transistor. *J. Semicond.* **2016**, *37*, 114003.
(27) Yuan, H.; Kwon, H.; Yeom, S.; Kwon, D.; Kang, S. MOSFET−BJT hybrid mode of the gated lateral bipolar junction transistor for C-reactive protein detection. *Biosens. Bioelectron.* **2011**, *28*, 434−437.
(28) Vanea, E.; Simon, V. XPS study of protein adsorption onto nanocrystalline aluminosilicate microparticles. *Appl. Surf. Sci.* **2011**, *257*, 2346−2352.
(29) Castner, D. G.; Hinds, K.; Grainger, D. W. X-ray photoelectron spectroscopy sulfur 2p study of organic thiol and disulfide binding interactions with gold surfaces. *Langmuir* **1996**, *12*, 5083−5086.
(30) Arvidsson, A.; Currie, F.; Kjellin, P.; Sul, Y.; Stenport, V. Nucleation and growth of calcium phosphates in the presence of fibrinogen on titanium implants with four potentially bioactive surface preparations. An in vitro study. *J. Mater. Sci.: Mater. Med.* **2009**, *20*, 1869−1879.
(31) Ahimou, F.; Boonaert, C. J. P.; Adriaensen, Y.; Jacques, P.; Thonart, P.; Paquot, M.; Rouxhet, P. G. XPS analysis of chemical functions at the surface of Bacillus subtilis. *J. Colloid Interface Sci.* **2007**, *309*, 49−55.
(32) Browne, M. M.; Lubarsky, G. V.; Davidson, M. R.; Bradley, R. H. Protein adsorption onto polystyrene surfaces studied by XPS and AFM. *Surf. Sci.* **2004**, *553*, 155−167.
(33) Serro, A. P.; Gispert, M. P.; Martins, M. C. L.; Brogueira, P.; Colaço, R.; Saramago, B. Adsorption of albumin on prosthetic materials: implication for tribological behavior. *J. Biomed. Mater. Res., Part A* **2006**, *78A*, 581−589.

DOI: 10.1021/acs.jafc.8b04455
J. Agric. Food Chem. 2018, 66, 11663−11671